

Research Article

Aditya Rio Prabowo*, Yuwana Sanjaya, and Fitrian Imaduddin

Forecasting technical performance and cost estimation of designed rim wheels based on variations of geometrical parameters

<https://doi.org/10.1515/jmbm-2022-0022>

received December 24, 2021; accepted May 13, 2022

Abstract: Rim wheel testing through the SAE standard is necessary for driving safety. This study focused on rim wheel tests carried out using the dynamic radial fatigue test method, which has been included in the SAE standard using Fusion360 for the design and ANSYS for the simulation. With different parameters for the rim wheel type, only some parameters of the tested rim wheels were able to pass the standardization by SAE; 16 rim wheels passed the test, while the other 11 rim wheels did not pass. Simulation results suggested that variations in the thickness, geometry, and material affected the displacement of the safety factor, which was inversely proportional. In addition, the variation in the rim wheel produced a change in the safety factor due to changes in its mass and cost, which were directly proportional. The results of this study will aid in rim wheel design, not only in terms of achieving the best performance but also with regard to cost efficiency.

Keywords: rim wheel, SAE, standard, parametric design

1 Introduction

In the automobile industry, the demand for energy saving and environmental protection is increasing, and the economic design of automobiles is attracting considerable

attention [1]. Today, the need for high mobility is increasing the demand for vehicles, and the use of cars is becoming essential. One of the most important components of a vehicle is the rim wheel because the vehicle cannot be driven without it [2]. A rim wheel is a circular component that can rotate on its axis, facilitating movement or transportation and supporting a load (mass) [3].

Car rim wheels play an important role in vehicle safety and performance. Rim wheel strength can maximize vehicle safety, but rim wheel mass and inertia can significantly reduce vehicle performance [4]. In actual conditions, there are still many rims that do not meet the standards; therefore, it is necessary to test rim wheels according to existing standards. Rim wheels can fatigue, resulting in failure such as cracks [5]. Therefore, standardized testing is carried out to meet a certain level of quality factors.

One of the standards used in fatigue testing is the SAE International standard. There are two main types of fatigue test methods: the dynamic radial fatigue test and the cornering fatigue test. Using test methods to design wheel fatigue is time- and cost-consuming [6]. Das [7] argued that the best practice for car wheels is to pass a dynamic radial fatigue test.

The test is usually carried out by machine testing; however, there is an alternative approach in the feasibility test, namely, through finite-element analysis (FEA). For this purpose, FEA is typically used during the design phase of product development [8]. In this study, ANSYS is used for static analysis because fatigue stress obtained from static stress analysis is reliable [9]. This simulation starts with the geometry with Fusion360 and continues with the static simulation on ANSYS. The simulation results are the structural response and safety factors for further analysis [10].

Rims that meet standards are built with ideal engineering analysis, where costs are usually not considered. Therefore, it is necessary to do a cost analysis, so that the rim that meets the standard can be produced with minimal cost. Karuppusamy *et al.* [11] only analyzed the

* **Corresponding author: Aditya Rio Prabowo**, Department of Mechanical Engineering, Universitas Sebelas Maret, Surakarta 57126, Indonesia, e-mail: aditya@ft.uns.ac.id

Yuwana Sanjaya: Department of Mechanical Engineering, Universitas Sebelas Maret, Surakarta 57126, Indonesia

Fitrian Imaduddin: Department of Mechanical Engineering, Universitas Sebelas Maret, Surakarta 57126, Indonesia; Department of Mechanical Engineering, Islamic University of Madinah, Medina 42351, Saudi Arabia

effect of different materials on rim strength. In this dynamic analysis, the results of statistical analysis and the best materials to make an effective rim structure were determined [12]. The results of this study will determine the best rim wheel design in terms of performance and cost-efficiency. Subsequently, we discuss the effect of rim strength according to SAE standards, after which the costs are analyzed to determine the rim performance that meets the standard with minimal cost.

2 Benchmarking study

This study uses static analysis of wheel rims as a benchmark, in which the data are provided from ANSYS simulations [2]. As shown in Figure 1, the design uses steel alloy with a total dimension of 450 mm × 300 mm. It consists of six-hole nuts (20 mm) with a thickness of 6 mm. The boundary condition is provided by the benchmark journal [11]. According to the benchmark journal, it has a load of 21.3 kN for each bolt hole, displacement (translation and rotation in x -, y -, z -directions are zero), and angular velocity (zero in x - and z -directions, and 62.8 rad/s in the y -direction is). The result of the benchmark study of the journal is shown in Table 1.

The benchmark method used is to vary mesh size from 5 to 60 mm within intervals of 5 mm. The mesh size variation is applied to the body of the rim wheel. It can be found that differences in meshing affected the parameters, which are nodes, elements, von Mises stresses, and displacements. The mesh convergence study with displacement ratio was obtained by plotting the displacement with the element length-to-thickness (ELT) ratio (Figure 2(a) and (b)). Meanwhile, the von Mises stress ratio is obtained by plotting the

Table 1: Properties of the material steel alloy on the benchmark journal

Material	Δx (mm)	$\sigma_{\text{von Mises}}$ (MPa)
Steel alloy	2.34×10^5	240

stress ratio with the ELT. From this convergence study, it can be concluded that the results are good at a mesh size of 20 mm, with an displacement error ratio of 0.938, error stress ratio of 0.936, and percentage of error ratio of 6.31%.

3 Research methodology

3.1 Design of rim wheel

The main purpose of the rim wheel structure is to ensure that all loads are distributed across the confluence of each part of the frame. This ensures that the rim wheel is not bent by force or restrained by bending loads [13]. The dimensions of the 2D design and 3D illustration of the rim wheel are shown in Figure 3(a) and (b).

The rim wheel of the vehicle was designed by TE37 Volkrays with a 9-18-H5 15/112.5/73 profile. The dimension was 9 × 18 in. (228.6 mm × 457.2 mm) with five holes, the diameter of the nut was 15 mm, the diameter of pitch circle diameter was 112.5 mm, and the diameter of the central hub was 73 mm. Three sizes of rim wheel thinness were used: 15, 17.5, and 20 mm. The geometry included three designs with four, five, and six spokes. At the same time, the type of material used in the rim wheel design included steel alloy, magnesium alloy, and aluminum

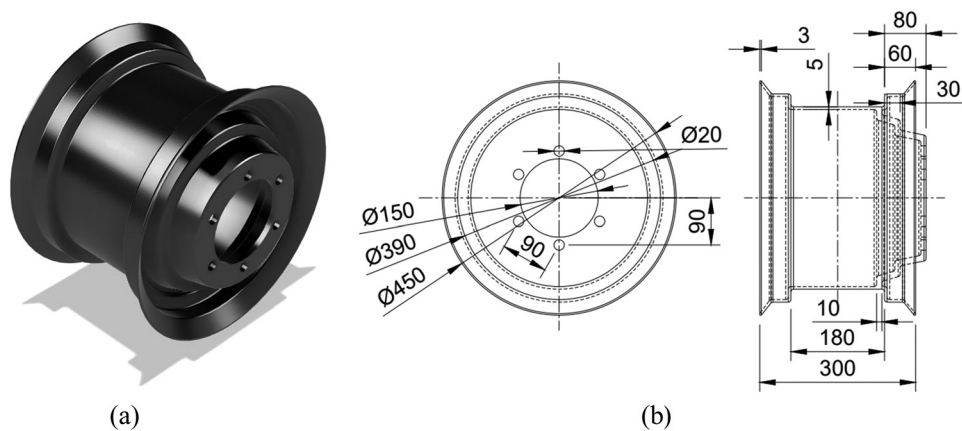


Figure 1: (a) Rim wheel design in 3D and (b) rim wheel design in 2D. All sizes are in mm.

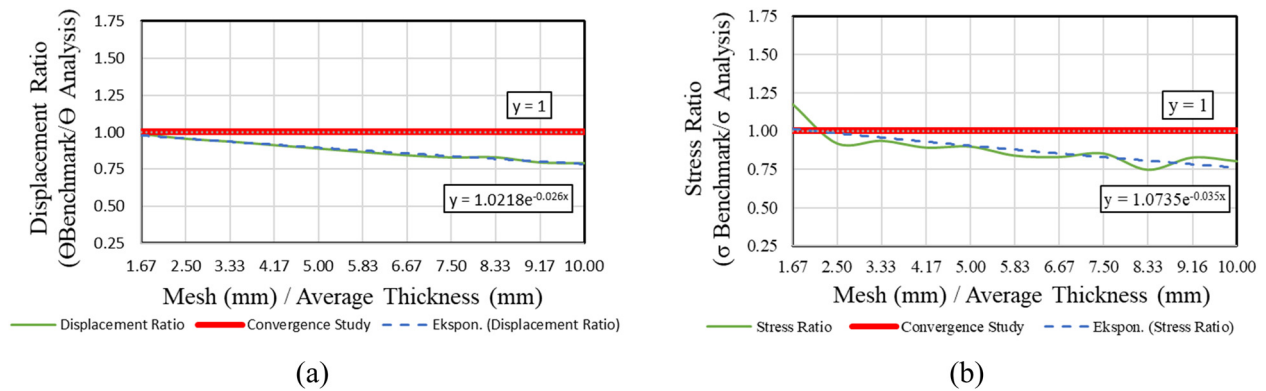


Figure 2: (a) Mesh convergence study with the displacement ratio and (b) mesh convergence study with the stress ratio.

alloy. This research was carried out with the variations shown in Table 2 and Figure 4.

three materials have different properties [15], as shown in Table 3.

3.2 Applied material

The materials used for the rim wheel in this study were steel alloy, magnesium alloy, and aluminum alloy. Steel alloy is made up of steel with a carbon content of $<0.25\%$, making it low-carbon steel. It also has the lowest cost compared to the other materials. Aluminum alloy has two important alloy compositions, namely Al (95.85–98.58%) and Si (0.4–0.8%), where silicon provides characteristics such as corrosion resistance. At last, magnesium alloys are alloys whose minimum magnesium content is 97%. Magnesium is the lightest structural metal due to its low density of 1.77 g/cm^3 [14]. The material cost is affected by the casting process in the manufacture of the rim wheel. With the casting process, the weight of the end material will be equal to the weight of the raw material used. These

3.3 Meshing configuration

All rim wheel variants were simulated using the same mesh parameters, namely, a standard 10-node mechanical tetrahedron. Other mesh parameters were set by default because different mesh densities were needed for each rim wheel depending on the frame's shape, structure, and material [16]. The 10-node tetrahedron mesh shape was chosen because it had excellent curve informing ability despite fewer knots. In addition, its accuracy remained high with simpler, lighter, and faster calculations. Convergence is only guaranteed if a static equilibrium line connects the solid states at the beginning and at the end of a time increment [17]. The size of the grid was designed based on the conclusions of the convergence.

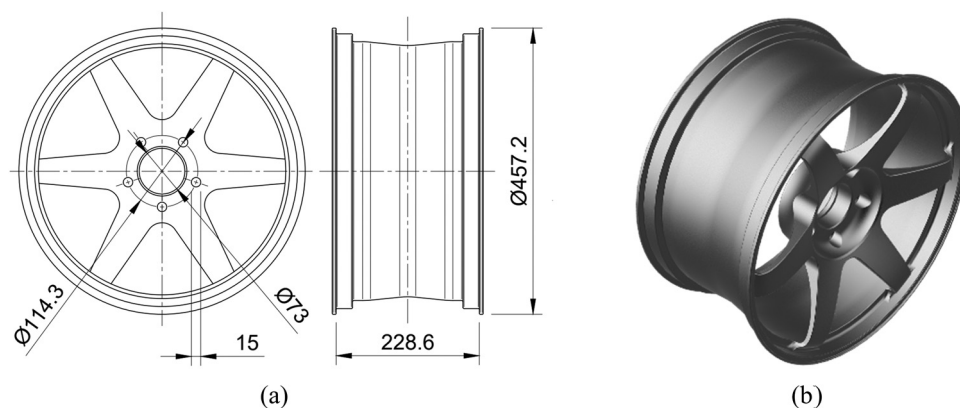











Figure 3: (a) Rim wheel design in 2D and (b) rim wheel in 3D. All sizes are in mm.

Table 2: Variations in designed rim wheels

		Number of spokes		
		4	5	6
Thickness	15 mm			
	17.5 mm			
	20 mm			

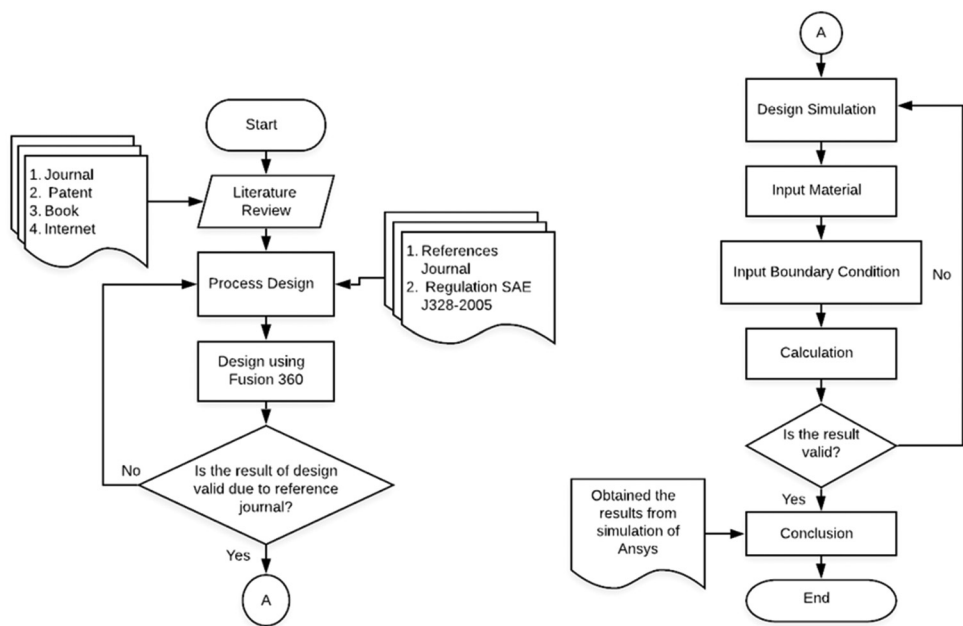


Figure 4: Research flow diagram.

3.4 Boundary condition

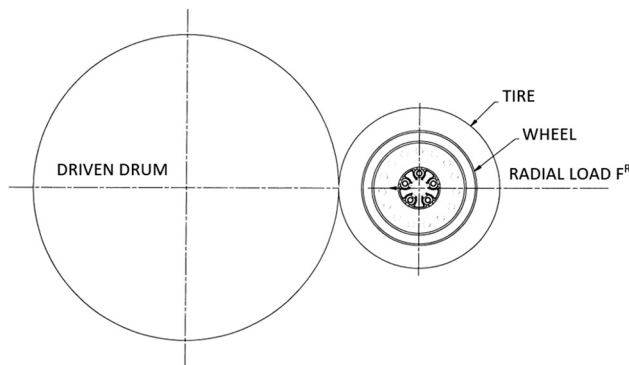
The SAE-recommended practice provides minimum performance requirements and unified procedure standardization of wheel fatigue testing for normal road traffic and

temporary use in passenger cars [18]. This study uses the dynamic radial fatigue test for simulations, as shown in Figure 5.

The procedure for this test is to use tires that are representative of the maximum size and with type 255/40 R18 [19].

Table 3: Properties of the materials

Material	Density (g/cm ³)	Modulus of elasticity (GPa)	Yield strength (MPa)	Tensile strength (MPa)	Callister cost (\$/kg)	Marketplace cost (\$/kg)
Steel alloy	7.85	207	250	460	1.45	1.022
Aluminum alloy	2.77	71	280	310	6.1	3
Magnesium alloy	1.8	45	193	255	8.8	8

**Figure 5:** Dynamic radial fatigue test [15].

The standard air pressure is 240 kPa for 690 kg maximum loads. Subsequently, the tire is mounted and inflated to 448 ± 14 kPa, with the wheels nuts tightened to 115 ± 7 N m. In the dynamic radial fatigue test, the load received by rim wheels and the length of the test are adjusted to the standards that have been set. The amount of radial load received can be formulated as follows:

$$F = W \cdot K, \quad (1)$$

where F is the radial loads, W is half of the maximum static load rating of the wheel as specified, and K is the load factor.

The maximum static load received by each wheel is 690 kg. At the same time, the magnitude of the load factor is different for each material used on the rim wheels. At SAE J 328, the load factor and the minimum cycle used during testing are set to obtain valid results. The magnitude of the load factor and minimum cycles are shown in Table 4.

3.5 Static and fatigue settings for ANSYS simulation

In this dynamic radial fatigue test simulation study, four loads are given to test the rim wheel. The loads include tire pressure, radial load, bolt tension load, and rim wheel rotational speed load. The amount of load given has been determined by the SAE standard.

According to SAE standards, the loading due to the tire pressure is 65 psi (0.448 MPa), with the direction of pressure on the entire outer surface of the rim to the flange. The maximum static load on passenger cars for the SNI standard tires is 690 kg or 6768.9 N, where the value of W is 3384.45 N. From this value, the radial load (F_r) on the rim wheel was calculated as 7615.0125 N for the value of Ferrous all ($K = 2.25$) and 8461.125 N for cast and forged aluminum ($K = 2.5$). The bolt tension specified by the SAE standard is 115 Nm. Before calculating the rotation of the rim wheel, it is known that the spindle speed is 237 rpm. As a result, the spindle has an angular velocity of 24.8 rad/s. The angular velocity of the rim wheel was obtained from the ratio of the angular velocity and diameter of the spindle and rim wheel, which is 50 rad/s. An example of static loading is shown in Figure 6.

Fatigue setting [20] in this case study aimed to determine the fatigue life and the area with the youngest age. Before starting the simulation, it was necessary to define fatigue tools to adjust the boundary conditions. In defining fatigue tools, Soderberg's theory was used with the assumption to determine the age of the rim wheel up to the yield strength point. The value of the ratio used was -1 , and the scale factor was 1, assuming that the loading was repeated according to the W load. From Figure 7, we can see the fatigue setting for the ANSYS simulation.

4 Comparative study for the radial dynamic fatigue test

Karuppusamy *et al.* [11] conducted a study to optimize fatigue on the rim wheel of four-wheeled vehicles using

Table 4: Test factor and minimum cycle requirements for wheels in normal highway service-dynamic radial fatigue

Rim wheel type (material)	"K" front	"K" rear	Minimum cycles
Ferrous all	2.25	2.0	400,000
Aluminum all	2.5	2.25	600,000

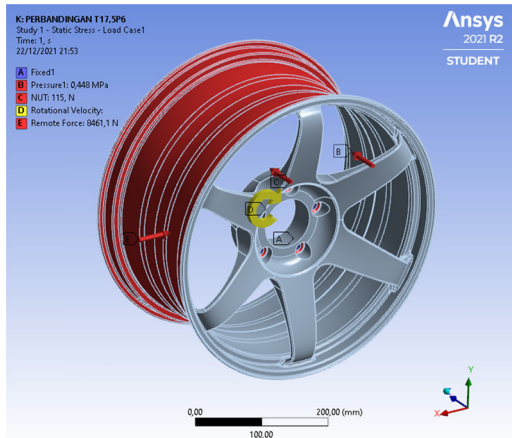


Figure 6: Static settings for ANSYS simulation.

the finite element method. The dimensions of the rim wheel were 450 mm outside diameter, 254 mm width, 20 mm bolt hole diameter, and 150 mm hub hole diameter. The materials used were steel alloy, aluminum alloy, magnesium alloy, and forged steel. Each material was tested using the radial dynamic fatigue test method. The fatigue produced on the steel alloy was 2.17×10^5 cycles, 1.32×10^5 cycles on the aluminum alloy, 1.2×10^5 cycles on the magnesium alloy, and 1.97×10^5 cycles on the forged steel. The results of the fatigue analysis obtained from four different materials showed that alloy steel is the best wheel rim material.

Shinde *et al.* [21] explained that reducing mass will reduce the total weight of the vehicle, which is related to

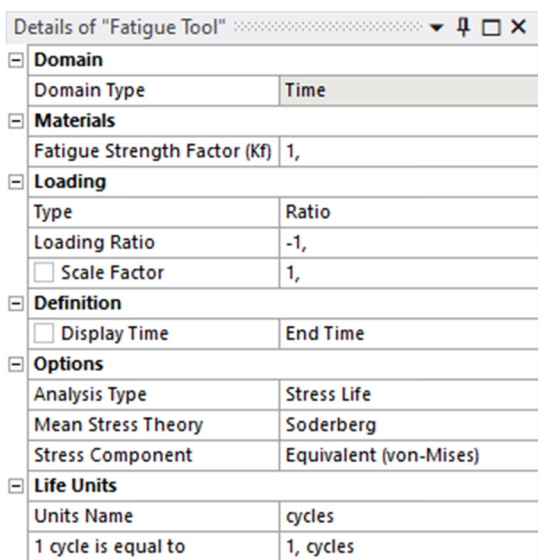
reducing production costs. The lower the weight of the vehicle, the better the fuel efficiency and performance. By analyzing the data from this reference, the fatigue value for four-wheeled vehicles can be determined. Therefore, the trend obtained from Karupusamy's research can be improved by varying the material, the number of bars, and the thickness to determine variations according to SAE International standards. As Sindhe's research showed that a reduction in mass would reduce production costs, a good rim wheel performance could be determined.

5 Results and discussion

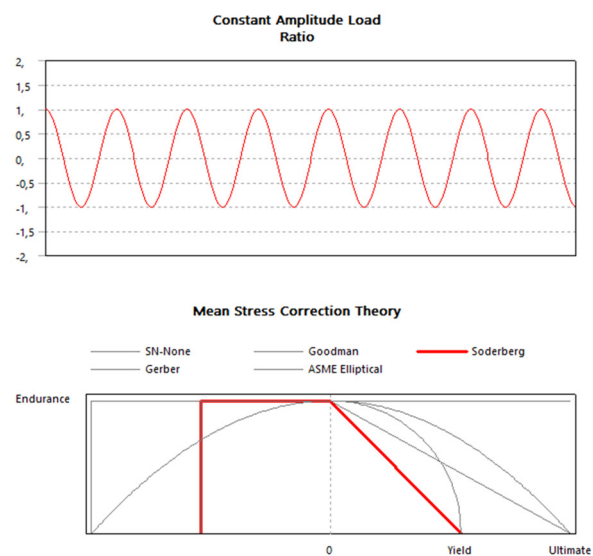
5.1 Structural response due to variations in material type

Gunawan *et al.* [22] stated that to avoid failure, the safety factor must be greater than 1.0; depending on the situation, the value of the safety factor was 1.0 to a little above 10. Three types of materials were used in this simulation were, namely, steel alloy (SA), magnesium alloy (MA), and aluminum alloy (AA). In this simulation, the structure of the rim wheel had a thickness (T) of 15, 17.5, and 20 mm, and the numbers of spokes (P) were 4, 5, and 6.

The naming of each variation has the following order: (material; SA, MA, AA) – P (number of spokes; 4, 5, 6) – T (thickness; 15, 17.5, 20)



(a)



(b)

Figure 7: Fatigue settings for the ANSYS simulation: (a) configuration in fatigue tool, and (b) assumed load ratio and mean stress.

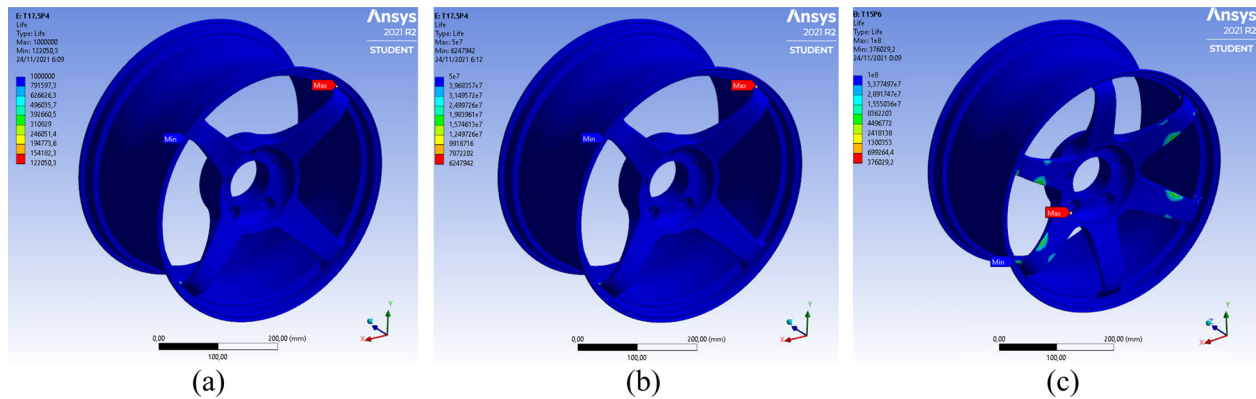


Figure 8: Variations of the rim wheel that experienced fatigue failure in the form of cracks: (a) SAP4T17.4; (b) MAP4T17.5; and (c) AAP6T15.

For example, the steel alloy with 4 spokes and a thickness of 15 mm is SAP4T15, the magnesium alloy with 5 spokes and a thickness of 17.5 mm is MAP5T17.5, and the aluminum alloy with 6 spokes and a thickness of 20 mm is AAP6T20.

Based on the SAE J 328 standard used in the dynamic radial fatigue test for passenger cars, the minimum fatigue life is 400,000 rounds for ferrous and 600,000 rounds for aluminum alloy. Meanwhile, the minimum fatigue life for some of these wheel designs is less than the minimum cycles. Three rim wheels with the steel alloy material, eight rims for the magnesium alloy, and five rims for the aluminum alloy passed the test. Meanwhile, 11 designs experienced fatigue failure caused by cracking before reaching the

minimum cycles value. Fatigue failure caused by cracks occurred at the edge of the rim. Some of the fatigue failure simulation results are shown in Figure 8.

Zhu *et al.* [23] conducted a study to meet the safety demands during operation. It is necessary not only to balance the strength and toughness of the wheels but also to have a complete understanding of the service conditions of the wheel materials.

In this study, the simulation results showed several designs fail to meet the standards. The failed designs are steel alloy materials under 400,000 cycles with 4 spokes for all thicknesses, 5 spokes for 15 mm thickness, and 6 spokes for 15 and 17.5 mm thicknesses; magnesium steel alloy material with 4 spokes for 15 mm thickness; and

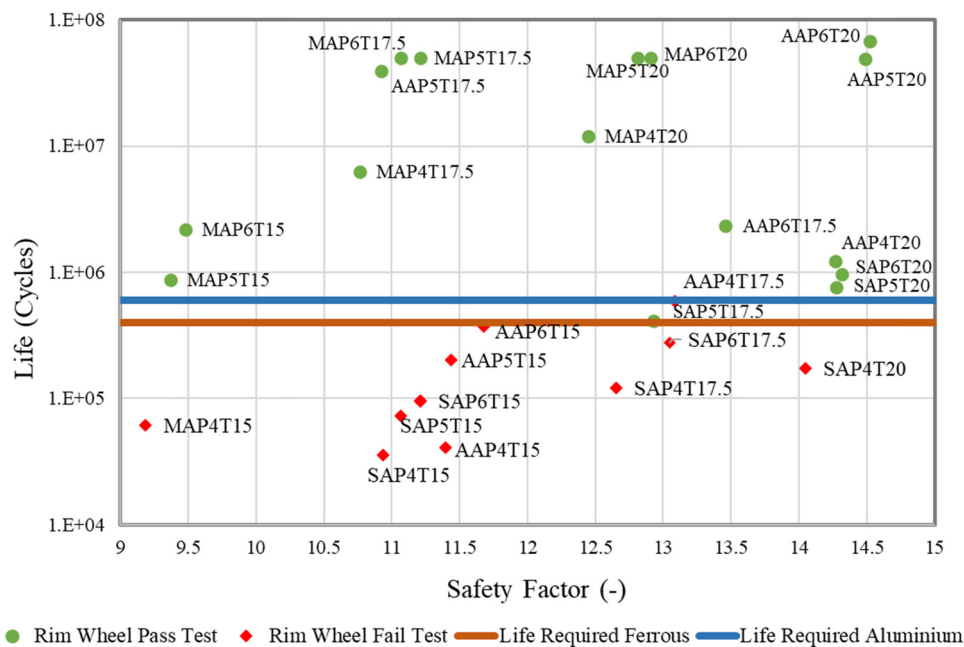


Figure 9: Rim wheel life due to the SAE standardization test.

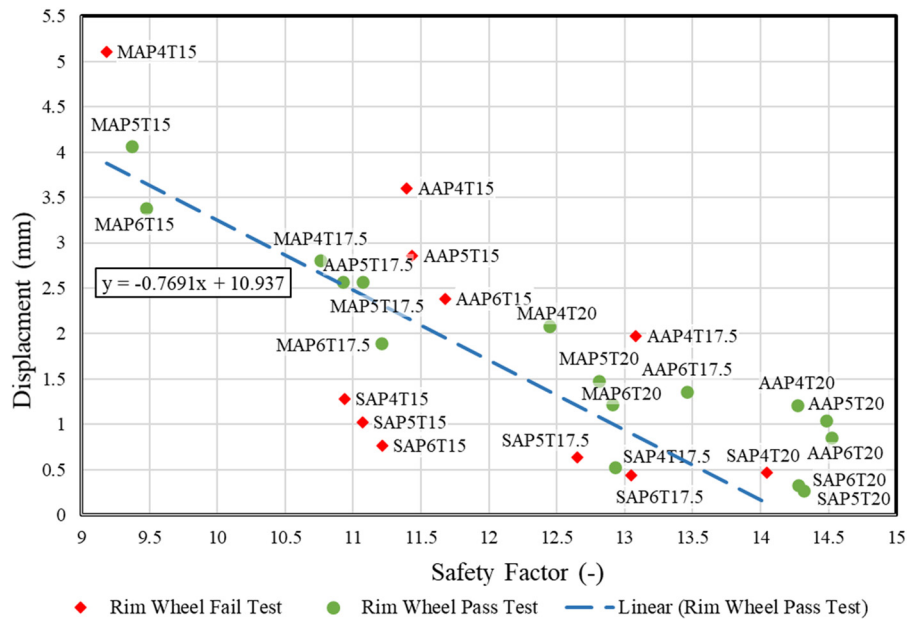


Figure 10: Response displacement due to the safety factor.

aluminum alloy under 600,000 cycles with 4 spokes for 15 and 17.5 mm thicknesses, 5 spokes for 15 mm thickness, and 6 spokes for 15 mm thickness. Eleven designs did not pass the SAE standard and the remaining 16 passed the test, as shown in Figure 9.

Aluminum material with 6 spokes and a thickness of 20 mm had a highest rim wheel life of 67,687,000 cycles, while steel alloy with 4 spokes and a thickness of 15 mm had the lowest rim wheel life is a life of 35,969 cycles. Eleven failed designs were caused by the cracks on the spoke ends, which resulted in the wheels undergoing permanent deformation before reaching their minimum cycle value. From Figure 9, the higher the life (cycles) on the rim wheel design, the higher the safety factor produced.

5.2 Structural response due to displacement

The displacement of the rim wheel structure is caused by radial load, nut load, and tire pressure. The value of the displacement of the structure must be less than the allowable displacement of the material. The results of the response deformation due to the safety factor of each simulation of deformation testing of the safety factor are shown in Figure 10.

Murugu Nachippan *et al.* [24] conducted a study in which general dimensions were controlled by decreasing the number of spokes with the same working characteristics and lower weight on the wheels. Different displacements could be seen from the six-spoke, five-spoke, and four-spoke wheels. However, the results of the number of

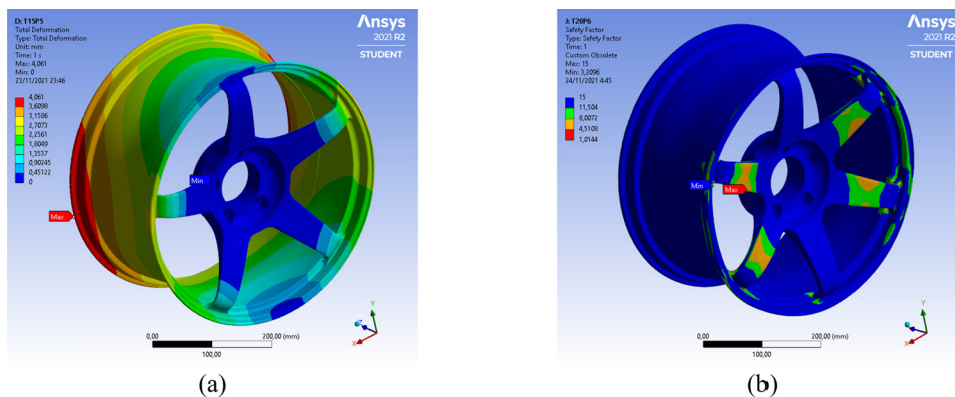


Figure 11: The highest value of displacement and safety factor: (a) MAP5T15 and (b) AAP5T15.

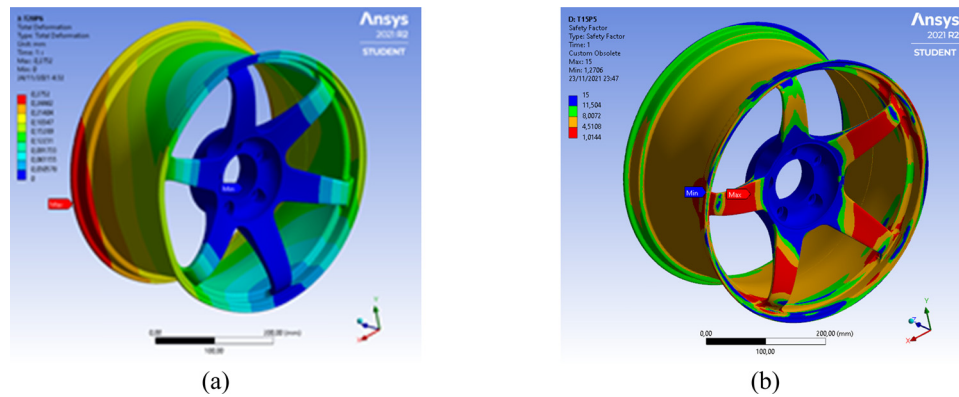


Figure 12: The lowest value of displacement and safety factor: (a) SAP6T20 and (b) MAP5T15.

bars could not be generalized to show which one is the best.

This study discusses the rim wheels that passed the SAE standardization test. Magnesium material with 5 spokes and a thickness of 15 mm has the highest rim wheel displacement of 4.061 mm; steel alloy material with 6 spokes and a thickness of 20 mm has the lowest rim wheel displacement of 0.275 mm. The highest rim wheel safety factor is 14.52, held by aluminum material with 6 spokes and a thickness of 20 mm, while the lowest rim wheel safety factor is 9.367, held by magnesium alloy material with 5 spokes and a thickness of 15 mm. The results of the highest and lowest displacement and safety factor simulations are shown in Figures 11 and 12.

From Figure 10, it can be seen that the largest displacement was found with the magnesium alloy, followed by the aluminum alloy and the steel alloy, which showed the lowest maximum displacement value. Moreover, Figure 10 shows that the effect of the displacement response on the safety factor is inversely proportional, i.e., the higher the displacement, the lower the safety factor, and *vice versa*.

The influence of mass also affects the safety factor. The simulation results showed that the steel alloy material has the heaviest mass of 26.543 kg. The magnesium alloy material has the lowest mass of 4.088 kg (Figure 10). The results of the mass response to the safety factor in each simulation are shown in Figure 13. Moreover, Figure 13

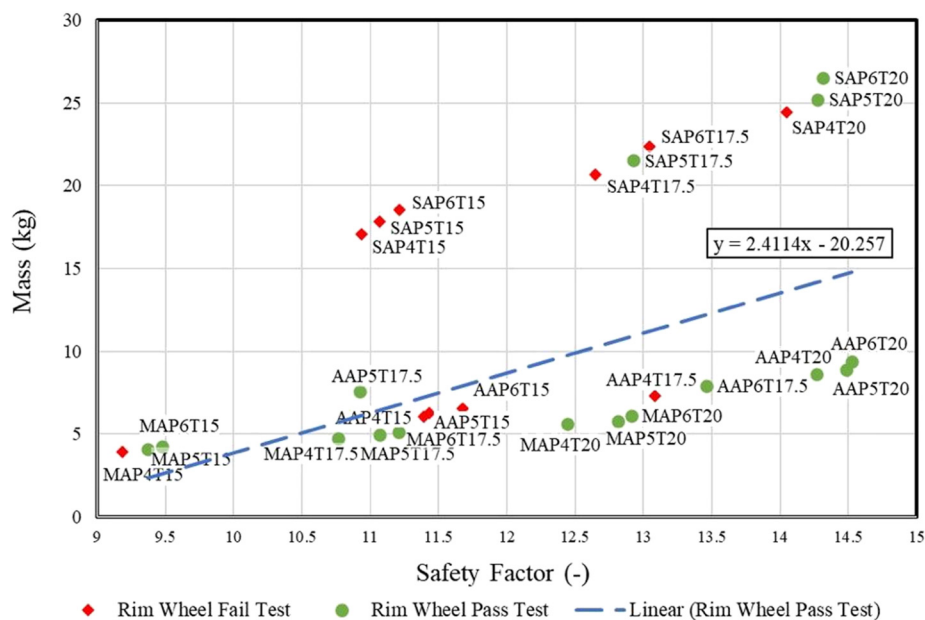


Figure 13: Response mass due to the safety factor.

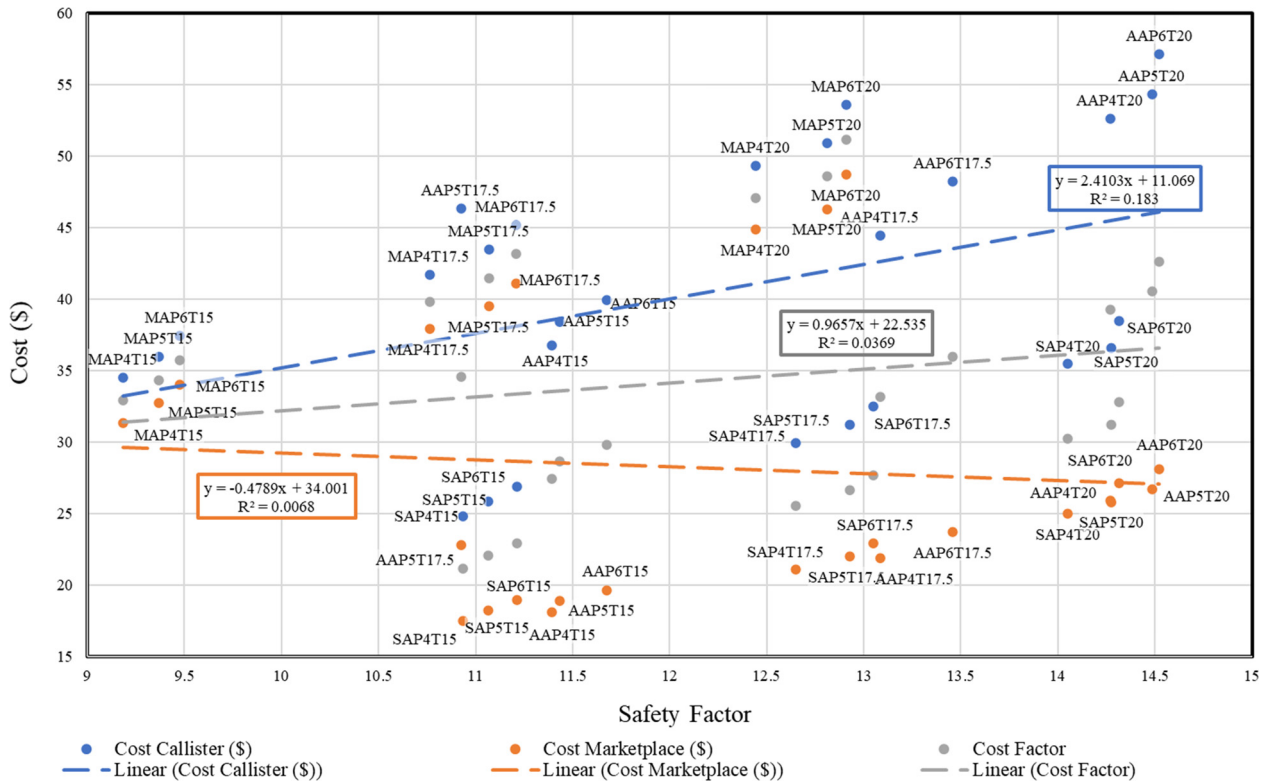


Figure 14: Impact of rim wheel cost on the safety factor (all costs are in US\$).

shows that the effect of mass on the safety factor is directly proportional, i.e., the lower the mass, the lower the safety factor, and *vice versa*.

5.3 Response of rim wheels to cost

This study had three variations in terms of material, geometry, and thickness. In this study, these three variations influenced the given cost. The costs incurred fluctuated; here, the average costs in the existing Callister book and the marketplace were taken [15]. The cost was obtained by multiplying the mass (kg) of each variation by the cost/mass (\$/kg) of the material, while the cost factor was obtained from the average of the cost for each variation in the cost results from the Callister book and the marketplace. Therefore, the average cost was calculated from these results to analyze the effect of costs on the safety factor. The graph of the impact of costs on the safety factor is shown in Figure 14.

From the graph, the magnesium alloy with 6 spokes and a thickness of 20 mm had the highest average cost of US\$ 51.13, while the lowest average price of US\$ 26.6 was seen for stainless steel with 5 spokes and a thickness of 17.5 mm. Figure 14 shows that the effect of cost on the

safety factor is directly proportional, i.e., the higher the cost, the higher the safety factor, and *vice versa*.

This cost estimation approach can be used for further analysis, especially in terms of critical transportations, such as ships, container trucks, liquefied natural gas carriers, etc. Performance is related to the mass, with the lightest mass seen with magnesium alloy, followed by aluminum alloy and finally steel alloy. However, in terms of cost, steel alloy had the lowest cost, followed by magnesium alloy, and the highest cost was for aluminum alloy. Considering the lowest mass and then the lowest cost, it can be seen that the magnesium alloy rim had the best performance, followed by steel alloy and finally aluminum alloy. In refs [25–31], the authors determined the needs of the components with consideration to the expected loads and casualties during their operations [32–36].

6 Conclusion

All variations in the test of the rim wheel structure were analyzed based on the effect of the response of the structure on the safety factor based on dynamic radial fatigue simulation tests. The following can be concluded:

1. The largest displacement occurred with magnesium alloy, followed by aluminum alloy and steel alloy, which had the lowest maximum displacement value. The effect of the displacement response on the safety factor was inversely proportional, i.e., the higher the displacement was, the lower the safety factor; conversely, the lower the displacement, the higher the safety factor.
2. The lightest mass was found for magnesium alloy, followed by aluminum alloy and steel alloy, which had the highest mass. The effect of mass on the safety factor was directly proportional, i.e., the lower the mass, the lower the safety factor, and *vice versa*.
3. The lowest cost was found for steel alloy, followed by magnesium alloy, and the highest cost was for aluminum alloy. The effect of cost on the safety factor was directly proportional, i.e., the higher the cost, the higher the safety factor, and *vice versa*.
4. Considering the lowest mass and then the lowest cost, it can be seen that the magnesium alloy rim that had the best performance, followed by the steel alloy rim and then the aluminum alloy rim.
5. The forecast of this analysis result could be improved by comparing the geometry with that of other materials using the comparative rim wheel designs in the market. Considering the mesh size, it is important to determine the range of mesh sizes first and then more accurately determine the mesh size. This will help authors evaluate the results of their simulations in a wider variety of ways.

Funding information: The article processing charge (APC) is supported by Universitas Sebelas Maret, Surakarta, Indonesia.

Author contributions: All authors have accepted responsibility for the entire content of this manuscript and approved its submission.

Conflict of interest: The authors state no conflicts of interest.

References

- [1] Jiang X, Lyu R, Fukushima Y, Otake M, Ju DY. Lightweight design and analysis of automobile wheel based on bending and radial loads. *IOP Conf Ser Mater Sci Eng.* 2018;372:372. doi: 10.1088/1757-899X/372/1/012048.
- [2] Sanjaya Y, Prabowo AR, Imaduddin F, Binti Nordin NA. Design and analysis of mesh size subjected to wheel rim convergence using finite element method. *Proc Struct Integr.* 2021;33:51–8. doi: 10.1016/j.prostr.2021.10.008.
- [3] Deepak SV, Naresh C, Hussain SA. Modelling and analysis of alloy wheel. *Int J Mech Eng Robot Res.* 2012;1:72–80.
- [4] Deka P, Bagherzadeh F, Murugesan S. Radial fatigue analysis of automotive wheel rim (ISO 3006). *Asian J Convergent Technol.* 2021;7:66–70. doi: 10.33130/ajct.2021v07i01.015.
- [5] Chilakala M, Garg S. Three dimensional numerical simulation of cracks in an automobile wheel rim. *Mater Today Proc.* 2019;26:2032–9. doi: 10.1016/j.matpr.2020.02.441.
- [6] Chen L, Li S, Chen H, Saylor D, Tong S. Study on the design method of equal strength rim based on stress and fatigue analysis using finite element method. *Adv Mech Eng.* 2017;9:1–11. doi: 10.1177/1687814017692698.
- [7] Das S. Design and weight optimization of aluminium alloy wheel. *Int J Sci Res.* 2014;4:1–12. doi: 10.29322/ijssr.
- [8] Soni D, Bhatt G. Static analysis of automotive wheel rim of different designs. *AIP Conf Proc.* 2020;2297:020014. doi: 10.1063/5.0029809.
- [9] Topaç MM, Günel H, Kuralay NS. Fatigue failure prediction of a rear axle housing prototype by using finite element analysis. *Eng Fail Anal.* 2009;16:1474–82. doi: 10.1016/j.engfailanal.2008.09.016.
- [10] Ary AK, Sanjaya Y, Prabowo AR, Imaduddin F, Nordin NAB, Istanto I, et al. Numerical estimation of the torsional stiffness characteristics on urban Shell Eco-Marathon (SEM) vehicle design. *Curved Layer Struct.* 2021;8:167–80. doi: 10.1515/cls-2021-0016.
- [11] Karuppusamy S, Karthikeyan G, Dinesh S, Rajkumar T, Vijayan V, Basha JK. Design and analysis of automotive wheel rim by using ANSYS and MSC fatigue software. *Asian J Res Soc Sci Humanit.* 2016;6:196. doi: 10.5958/2249-7315.2016.01007.8.
- [12] Vijayakumar R, Ramesh C, Boobesh R, Ram Surya R, Souder Rajesh P. Investigation on automobile wheel rim aluminium 6061 and 6066 Alloys using ANSYS WORKBENCH. *Mater Today Proc.* 2020;33:3155–9. doi: 10.1016/j.matpr.2020.03.798.
- [13] Ballo F, Previati G, Mastinu G, Comolli F. Impact tests of wheels of road vehicles: A comprehensive method for numerical simulation. *Int J Impact Eng.* 2020;146:103719. doi: 10.1016/j.ijimpeng.2020.103719.
- [14] Sharma A, Yadav R, Sharma K. Optimization and investigation of automotive wheel rim for efficient performance of vehicle. *Mater Today Proc.* 2021;45:3601–4. doi: 10.1016/j.matpr.2020.12.1110.
- [15] Callister WD, Wiley J. *Materials science and engineering an introduction.* 8th ed. New Jersey: John Wiley & Sons Inc; 2009.
- [16] Vangi D. *Structural behavior of the vehicle during the impact. Vehicle Collision Dynamics.* Oxford: Butterworth-Heinemann; 2020.
- [17] Gao YF, Bower AF. A simple technique for avoiding convergence problems in finite element simulations of crack nucleation and growth on cohesive interfaces. *Model Simul Mater Sci Eng.* 2004;12:453–63. doi: 10.1088/0965-0393/12/3/007.
- [18] SAE. *Wheels-passenger car and light truck performance requirements and test procedures.* Vol. 2. SAE J328. SAE International: Surface Vehicle Recommended Practice; 2005.
- [19] SNI. *Passenger car tires.* 98th ed. National Standardization Agency. Standar Nasional Indonesia; 2019. p. 27.

- [20] Fajri A, Prabowo AR, Surojo E, Imaduddin F, Sohn JM, Adiputra R. Validation and verification of fatigue assessment using FE analysis: A study case on the notched cantilever beam. *Proc Struct Integ.* 2021;33:11–8. doi: 10.1016/j.prostr.2021.10.003.
- [21] Shinde T, Jomde A, Shamkuwar S, Sollapur S, Naikwadi V, Patil C. Fatigue analysis of alloy wheel using cornering fatigue test and its weight optimization. *Mater Today Proc.* 2022. doi: 10.1016/j.matpr.2022.02.023.
- [22] Gunawan Y, Samhuddin, Masud F, Endriatno N, Yamin M, Muslimin. Design and load analysis toward the strength of rim modification using solidworks software on motorcycle as a city transportation. *Proceedings of the 2nd International Symposium on Transportation Studies in Developing Countries (ISTSDC 2019)*; 2020. p. 77–81. doi: 10.2991/aer.k.200220.016.
- [23] Zhu Z, Zhu Y, Wang Q. Fatigue mechanisms of wheel rim steel under off-axis loading. *Mater Sci Eng A.* 2020;773:138731. doi: 10.1016/j.msea.2019.138731.
- [24] Murugu Nachippan N, Backiyaraj A, Navaneeth VR, Maridurai T, Vignesh M, Vijayan V, et al. Structural analysis of hybridized glass fiber hemp fiber reinforced composite wheel rim. *Mater Today Proc.* 2020;46:3960–5. doi: 10.1016/j.matpr.2021.02.496.
- [25] Krikis RN, Wang B, Niotis S. An analysis of the ballast voyage of an LNG Carrier. The significance of the loading and discharging cycle. *Appl Therm Eng.* 2021;194:117092. doi: 10.1016/j.applthermaleng.2021.117092.
- [26] Smaradhana DF, Prabowo AR, Ganda ANF. Exploring the potential of graphene materials in marine and shipping industries – A technical review for prospective application on ship operation and material-structure aspects. *J Ocean Eng Sci.* 2021;6:299–316. doi: 10.1016/j.joes.2021.02.004.
- [27] Prabowo AR, Tuswan T, Prabowoputra DM, Ridwan R. Deformation of designed steel plates: An optimisation of the side hull structure using the finite element approach. *Open Eng.* 2021;11:1034–47. doi: 10.1515/eng-2021-0104.
- [28] Akbar MS, Prabowo AR, Tjahjana DDDP, Tuswan T. Analysis of plated-hull structure strength against hydrostatic and hydrodynamic loads: A case study of 600 TEU container ships. *J Mech Behav Mater.* 2021;30:237–48. doi: 10.1515/jmbm-2021-0025.
- [29] Zhang R, Yun WY, Moon I. A reactive tabu search algorithm for the multi-depot container truck transportation problem. *Transp Res Part E Logist Transp Rev.* 2009;45:904–14. doi: 10.1016/j.tre.2009.04.012.
- [30] Nossack J, Pesch E. A truck scheduling problem arising in intermodal container transportation. *Eur J Oper Res.* 2013;230:666–80. doi: 10.1016/j.ejor.2013.04.042.
- [31] Ding S, Wang G, Luo Q. Study on sloshing simulation in the independent tank for an ice-breaking LNG carrier. *Int J Nav Archit Ocean Eng.* 2020;12:667–79. doi: 10.1016/j.ijnaoe.2020.03.002.
- [32] Widiyanto I, Alwan FHA, Mubarak MAH, Prabowo AR, Laksono FB, Bahatmaka A, et al. Effect of geometrical variations on the structural performance of shipping container panels: A parametric study towards a new alternative design. *Curved Layer Struct.* 2021;8:271–306. doi: 10.1515/cls-2021-0024.
- [33] Wang J, Yi B, Zhou H. Framework of computational approach based on inherent deformation for welding buckling investigation during fabrication of lightweight ship panel. *Ocean Eng.* 2018;157:202–10. doi: 10.1016/j.oceaneng.2018.03.057.
- [34] Sonsino CM, Breitenberger M, Krause I, Pötter K, Schröder S, Jürgens K. Required Fatigue Strength (RFS) for evaluating of spectrum loaded components by the example of cast-aluminum passenger car wheels. *Int J Fatigue.* 2021;145:145. doi: 10.1016/j.ijfatigue.2020.105975.
- [35] Prabowo AR, Tuswan T, Nurcholis A, Pratama AA. Structural resistance of simplified side hull models accounting for stiffener design and loading type. *Math Probl Eng.* 2021;2021:19. doi: 10.1155/2021/6229498.
- [36] Prabowo AR, Tuswan T, Adiputra R, Do QT, Sohn JM, Surojo E, et al. Mechanical behavior of thin-walled steel under hard contact with rigid seabed rock: Theoretical contact approach and nonlinear FE calculation. *J Mech Behav Mater.* 2021;30:156–70. doi: 10.1515/jmbm-2021-0016.